UCRL-92648
PREPRINT

AN IMPROVED PARTICLE-VELOCITY TRANSDUCER FOR EQUATION-OF-STATE EXPERIMENTS

Sam J. Spataro

This paper was prepared for submittal
to the 13th Transducer Workshop
Monterey, California
June 4-6, 1985

May 30, 1985

Lawrence Livermore National Laboratory

DISCLAIMER

AN IMPROVED PARTICLE-VELOCITY TRANSDUCER FOR EQUATION-OF-STATE EXPERIMENTS *

Sam J. Spataro

University of California
Lawrence Livermore National Laboratory
Livermore, California

ABSTRACT

An improved particle-velocity transducer has been developed for use in equation-of-state experiments in the low (sub-kilobar) shock region. In low amplitude shock experiments, our standard one-turn transducer generated voltages so low that signal-to-noise problems were limiting our resolution. By using multiple turns in the new transducer, we get an increase in signal, proportional to the number of turns, with no apparent increase in noise.

The complete experiment system consists of passive, multiple-turn current-loop transducers, a Helmholtz pair of electromagnets, a firing and timing system, a data recording system, the material under study, and a small explosive charge.

Each current "loop" is actually a narrow linear strip (or element) of very thin copper foil, which is embedded in the test material. The shock wave from the emplaced explosive charge moves the element across an orthogonal magnetic field causing, for a brief period, a voltage output proportional to the velocity of the element.

In this paper I present the theory and design of a new three-turn transducer, its advantages, its error sources, and some typical test results. Also, I will briefly describe the magnetic field generator, the data recording system, and data processing.

---

*Work performed under the auspices of the U.S. Department of Energy by the Lawrence Livermore National Laboratory under contract No. W-7405-ENG-48.

INTRODUCTION

The objective of the equation-of-state (EOS) work at the Lawrence Livermore National Laboratory (LLNL) (Ref. 1) is to provide a data base for material response modeling and computer code development, and to test dimensional similarity for small-size to field-size experiments. This work has direct application in the LLNL Containment Program, Seismic Monitoring Program, Ice Penetration Program, and similar areas of research.

We have, for a number of years, conducted the EOS experiments using a single-turn passive transducer to measure particle velocity. We have recently developed an improved particle-velocity transducer for use in EOS experiments in the low (sub-kilobar) shock region.

The complete EOS instrumentation system (Fig. 1) consists of (1) ten or more passive multiple-turn current-loop transducers embedded in the material under study, (2) a Helmholtz coil pair of electromagnets to establish a magnetic field perpendicular to the transducer element and its motion, (3) a firing and timing system, (4) a data recording system, (5) a block of the material under study, and (6) a small explosive charge with a mild detonating fuse.

Each single-turn current loop, or element, is a narrow, linear strip of copper foil. The multiple-turn transducer provides an electrical signal that is proportional to the velocity at which a single-turn loop, embedded in the material under study, moves through the DC magnetic field. The transducer is moved through the field by a shock wave created by detonating the charge of chemical explosive emplaced in the material. By exciting the material with a shock from an explosive source, we obtain the time history representation of <u>in-situ</u> particle velocity that the embedded gage sees as it moves with the material. This method has been successfully used to measure dynamic loading and unloading of material to describe their EOS.

Standard time delays, synchronizing pulses, and fiducial markers, all accurately timed, are included in the overall measuring system to ensure synchronization of sweep time and signal arrival. The firing and timing system, as well as the data recording system, is illustrated in Fig. 2.

The data recording system consists of precision oscilloscopes and high-speed cameras to record the voltage output waveform as a function of time. The recorded trace is digitized, transferred to magnetic tape, and then input to a computer for standard processing. The reduced data includes displacement, acceleration, and spectral information.

The reason for developing the improved transducer was that in recent investigations of very low (sub-kilobar) shocks, our standard one-turn transducer generated voltages so low that signal-to-noise problems were limiting signal resolution. Our new three-turn transducer overcomes this problem efficiently and economically. By using multiple turns, we obtain an increase in signal proportional to the number of turns with no apparent increase in noise.

THEORY OF OPERATION

The principle of operation for the transducer is governed by Faraday's Law (and is represented for our purposes in Figs. 3 and 4): i.e., the motion of a conductor in a magnetic field produces a voltage that is proportional to the velocity of the conductor. Mathematically.

$$\vec{V} = (\vec{B} \times \vec{u}) \cdot \vec{\ell} \, ,$$

where,

V = output voltage (volts)

B = magnetic field (webers/m^2)

u = velocity (m/sec)

ℓ = length of element (meters).

When $\vec{B}$, $\vec{u}$, and $\vec{\ell}$ are mutually orthogonal, as they are in our experiments, the output voltage, V, is the scalar product of the three parameters. With B and ℓ known, V is then proportional to the velocity, u.

The distance traveled, Δx, of the element, ℓ, is very small, typically in the 100-microinch range. This very small travel assures us of a straight-line motion through the field, B, precluding any curved-path corrections.

The Lorentz force from the magnetic field acts on free charges within the metallic conductor (loop) to establish a voltage that is a function of the net charge motion. The relationship of voltage and velocity is derived from Faraday's induction law:

$$\phi = \oint \vec{B} \cdot dA \quad , \tag{1}$$

which reduces to

$$\phi = B \cdot A \quad .$$

It states that when there is a change in magnetic flux, ϕ, an electromotive force is established either by a change of the magnetic field, B, or by a change in the area, A, swept by the element, ℓ. This induced voltage, V, is proportional to the rate of change in net flux. That is,

$$V = -n \frac{d\phi}{dt} \quad , \tag{2}$$

where n = number of turns in the loop. The negative sign refers to the sense of V due to a collapsing field.

Combining Equations (1) and (2) we have

$$V = -n \frac{d}{dt} (B \cdot A)$$

$$= -n \frac{d}{dt} (B \cdot \ell \, dx) \quad .$$

Finally,

$$V = -n \cdot B \cdot u \cdot \ell \, ,$$

where $u = \dfrac{dx}{dt}$ (3)

We see, then, that we can achieve an increase in transducer sensitivity by merely increasing the number of turns, n.

THE TRANSDUCER

The previously used single-turn transducer and the new three-turn unit are shown pictorially and schematically in Fig. 5. Both transducers are fabricated from copper foil ($\approx$1 mil thick) sandwiched between layers of 2 mil

Kapton, a transparent Mylar-type material. The Kapton acts as an insulator and also adds strength to the unit. The copper and Kapton are bonded with an epoxy resin approximately 0.1 mil thick.

The individual elements of the three-element unit are jumpered at their far ends so that the three loops are electrically in series. Care is taken to ensure that the jumpered end is sufficiently removed in distance from the active end so that there is no motion during the time the transducer is returning useful data.

The transducer leads are soldered to the center conductor and shield of RG-174/U, 50 ohm coaxial cable. The cable is then patched to RG-8/U coaxial cable, which completes the run to the oscilloscope/camera system.

In the original single-turn transducer, the element length was chosen to optimize signal output (V is proportional to ℓ), and the "geometric resolution" of the transducer. The geometric resolution is the transit time, t, of a circular shock front sweeping across the active element, ℓ. This time is a function of (1) the distance between the shock origin and transducer, (2) the shock velocity, v, and (3) the separation between lead wires, ℓ. The time for the shock wave to totally engulf the element tends to "smear" the particle-velocity measurement across the element.

From the geometry in Fig. 6,

$$r^2 = (r - h)^2 + \left(\frac{\ell}{2}\right)^2 \quad ,$$

where $h = v \cdot t$, from which

$$t = \frac{r - 0.5\ (4r^2 - \ell^2)^{1/2}}{v} \quad . \qquad (4)$$

If we assume a transducer-to-explosive separation of $r = 200$ mm, $\ell = 9$ mm, $v = 3 \times 10^3$ m/sec, then the foil is engulfed in $\approx$17 ns. This time is some 2 orders of magnitude faster than the rise time of the particle-velocity pulse. Hence, there is little smearing of the velocity signal.

For the shock radii and velocities used in our experiments, $\ell = 9$ mm is an optimum transducer element length.

ERROR SOURCES

It is not the intent of this paper to engage in a formal, quantitative error analysis. Rather, I point out here some of the errors we are aware of that reside in both the old and new three-turn transducer system. Overall, we have a system accuracy of $\approx 2\%$.

There are several sources of possible measurement error common to both the single-turn and three-turn transducer:

(1) The geometric resolution, mentioned above, results in an integrated measurement of u <u>across</u> the gage element and not at a point. This error, measured by the transit time, t, is of the order of 10 to 50 ns.

(2) If the leads between the element, ℓ, and the signal cable are not parallel to the magnetic field, we can get contributions due to the leads moving through the field. This is minimized by offsetting the transducer so it does not straddle the geometric center of the field (Ref. 2). Figure 7 is a pictorial representation of this problem.

(3) The three individual loops must be connected beyond the point of any movement so that we maintain the X3 gain.

(4) A "thick" transducer (the overall dimension, including copper and kapton) yields unwanted signals due to reflections off the transducer/material interface. The three-turn transducer is overall less than 12 mils in thickness, and the error contribution from this source is small.

(5) There are errors of a lesser magnitude due to: nonhomogeneous magnetic field, transducer element stretching after shock impact, signal cable noise, and the Johnson noise of the transducer itself.

THE HELMHOLTZ MAGNETS

The DC magnetic field, which supplies the Lorentz force for the transducer, is generated by a Helmholtz coil pair. We have two such magnets--a small and a large--and a brief description of each is given in Table 1. (The small magnet is described in greater detail in Ref. 3.)

The small magnet is water cooled, and can handle about 1500 amperes (maximum) for an extended length of time. (This current yields about 2.5 kgauss.) Power consumption at this level is 200 kW.

The large magnet has been operated at 800 amperes, with field level at about 2 kgauss. Power consumption is 270 kW. A dual ranged, constant-current power supply, rated at 600 kW, supplies the current to both of these magnets.

THE DATA RECORDING SYSTEM AND DATA REDUCTION

Data from the transducer is recorded on Tektronix 7000 series oscilloscopes with 200 MHz band widths (see Fig. 2). Both the horizontal and vertical amplifiers are calibrated with frequency and voltage standards after every experiment.

Standard high-speed Polaroid film is used with the camera. The film is then photo enlarged to approximately 8x10 inches, and the trace is manually digitized and recorded on magnetic tape.

The tape is then interfaced to a Prime 750 computer where standard processing is done. Some of the data processing includes integration and differentiation of the velocity data to yield displacement and acceleration, and fast Fourier transforms for spectral information.

A hardcopy of the processed data is the final output. Figures 8 and 9 are typical data from our three-turn transducer.

FURTHER WORK

We are presently procuring and will soon evaluate a high speed (CAMAC) transient digitizing system that will be interfaced to either an LSI-11 computer or a personal computer. This will ultimately replace the oscilloscope/camera systems and will allow us near-real-time data processing capability. With 10-bit dynamic range and 10-MHz bandwidths, we can record very fast data with about an order-of-magnitude improvement in resolution over our existing oscilloscope/camera system.

We are planning some future development on n-turn units to get even more sensitivity and less unwanted signals:

(1) We are looking at thinner insulating material and vapor depositions so we can approach 3 to 4 mil total thickness.

(2) We have built and have done some limited testing on a five-turn transducer that has five times the sensitivity over our previous transducer, with no increase in noise.

(3) We are considering a design that would have an increase in sensitivity of X12

CONCLUSIONS

We have designed and used in approximately twenty-five measurements an improved particle velocity transducer for EOS work. The advantages of this three-turn transducer over our previous single-turn transducer are:

- Three times the output with no discernible noise increase.
- No change is required in our data system.

ACKNOWLEDGEMENT

The author wishes to acknowledge Don Larson, LLNL physicist, who enthusiastically accepted the idea of the new transducer design and coordinated efforts to get it fabricated, tested, and used in his experiments. His timely comments, suggestions, and critique of this paper were very helpful.

REFERENCES

1. Don Larson, private communication, Lawrence Livermore National Laboratory, Livermore, California.
2. H. C. Rodean, D. B. Larson, J. R. Hearst, and S. R. Brown, ARPA-AEC Seismic/Evasion Research Program: Progress on Small-Scale HE Experiments and Computer Code Verification, Lawrence Livermore National Laboratory, Livermore, California, July 27, 1970.
3. Sam Spataro, Design of a Helmholtz-type Magnet for Equation-of-State Experiments, Lawrence Livermore National Laboratory, Livermore, California, Internal Report LER 70-105201, December 1970.

Table 1. Important features of the two Helmholtz coil pair of electromagnets available for EOS experiments.

Parameter	Small magnet	Large magnet
Mean diameter of coils	56 cm	230 cm
Gap spacing	Variable to 45 cm	100 to 150 cm
Field strength, kgauss	Variable to 2.5 kgauss (to 0.25 weber/m^2)	2.5 kgauss (nominal)
Homogeneity of field at geometric center of magnet	<1% over 150 cm^3; <0.5% over 100 cm^3	0.5% over a large volume
Ripple in field	<1% variation, long term	<1% variation
Portability	Easily moved with forklift	Permanently mounted

FIGURE CAPTIONS

Figure 1. A typical "shot" setup, with the material under study placed within the polegap of a magnet. The transducer is set up to measure in-situ particle velocity. The explosive is detonated at "zero-time," with all timing for the measurement system referenced to that time. In reality, we may have ten or more transducers at various radii from the charge, along with associated timing equipment and oscilloscope/camera systems.

Figure 2. Diagram of the firing and timing system and the data recording system. The test sequence is initiated manually with the firing switch. A pulse from the detonator pulser is sent to both the explosive charge and the timing circuits to ensure accurate synchronization of oscilloscope sweep time, signal arrival, and camera-shutter activation. The waveforms on the oscilloscopes are recorded on high-speed film.

Figure 3. Pictorial representation of the transducer element, ℓ, moving through a distance, dx, in a magnetic field, B. The rate of motion of the element, dx/dt, is the in-situ particle velocity, u, of the transducer and material. The three-turn transducer is three of these loops connected in series to give a gain of X3.

Figure 4. Vector diagram for the three main parameters of the EOS experiments. Great care is taken to ensure that the three vectors, $\vec{u}$, $\vec{B}$, and $\vec{\ell}$, are orthogonal. When this is true, the output voltage developed across element, ℓ, is simply the scaler product of the parameters; that is $V = -B \cdot \ell \cdot u$.

Figure 5. The previous standard transducer and the new three-turn unit, shown both pictorially and schematically. Both are constructed of the same materials. The three-turn unit is simply three single-turn units laid one on the other and electrically connected in series. The impedance of the transducer is in the milliohm range.

Figure 6. Diagram illustrating the parameters that describe the geometric resolution, which is the travel time, t, of a circular shock wave front with velocity v sweeping across the transducer active element, ℓ. The radius of curvature of the shock front is r. The parameter h is the distance the shock front travels from first contact to total engulfment of the transducer element.

Figure 7. Explanation of method of compensating for nonparallel magnetic field by offsetting transducer from center of field. The B_y components of the nonuniform field through which these transducers move induce unwanted voltages in each of the leads. In transducer 1, both unwanted lead voltages add to the desired signal voltage, but in Transducer 2, one adds and the other subtracts. In the magnetic system now being used, the contributions from the leads in the Transducer 1 configuration represent about 5% of the signal. For the Transducer 2 configuration, however, the field orientation is such that no contribution is detected.

Figure 8. A typical particle-velocity time history. These signals were obtained from two transducers positioned side by side in compacted dirt, 70 mm from the center of a small explosive charge. The data scatter is typical of any transducer pair in pressed dirt.

Figure 9. Typical suite of particle-velocity time histories. This ensemble of particle-velocity measurements is one form of data presentation. Displayed in this manner, one can easily see the delay in shock arrival times, the decay in amplitudes, and the slower rise times--all with increasing distances between the transducers and the chemical explosive charge.

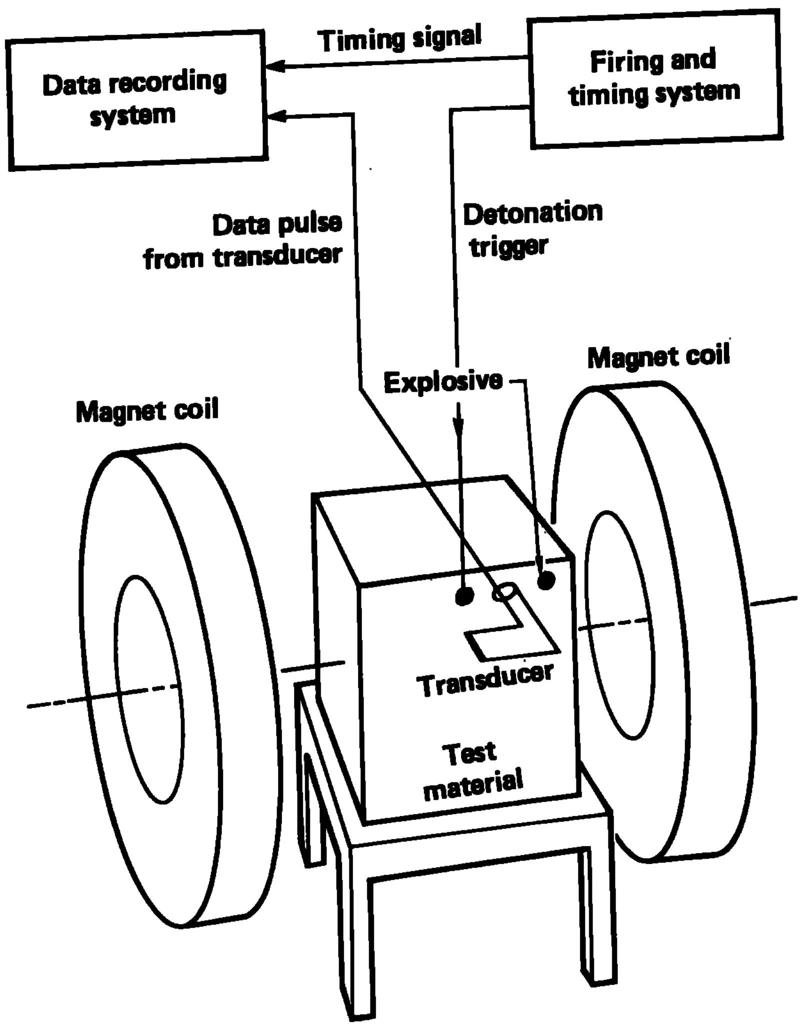

Spataro — Fig. 1

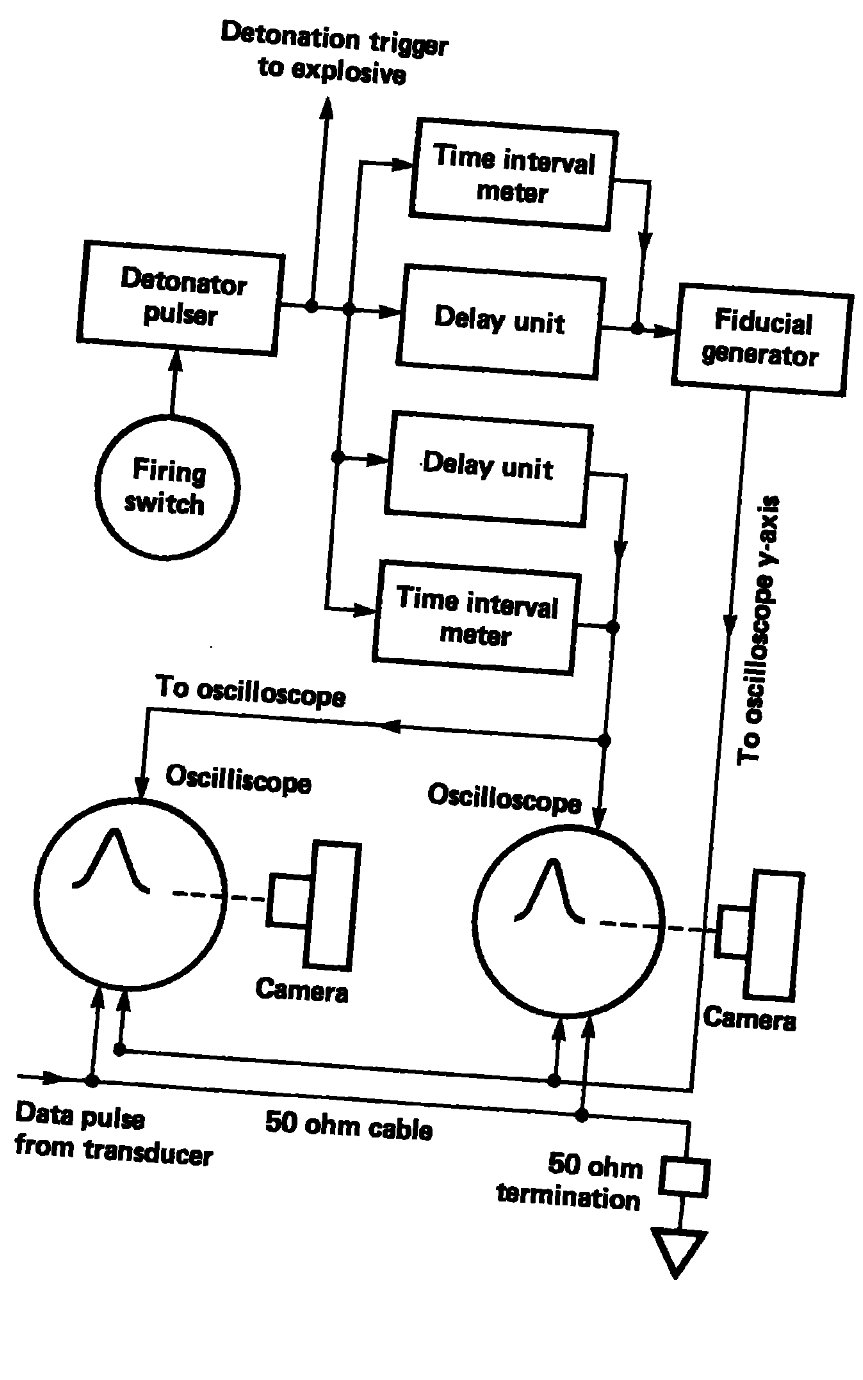

Spataro — Fig. 2

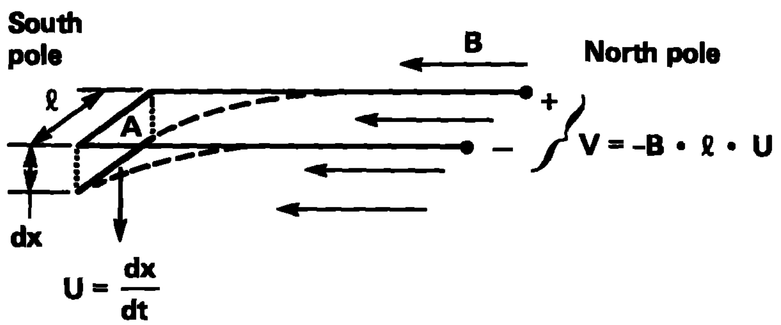

Spataro — Fig. 3

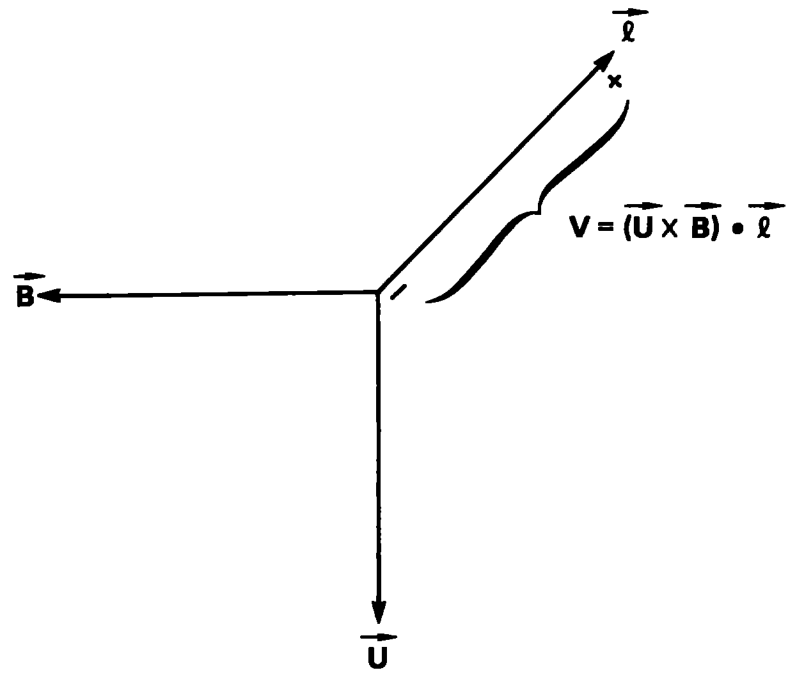

Spataro — Fig. 4

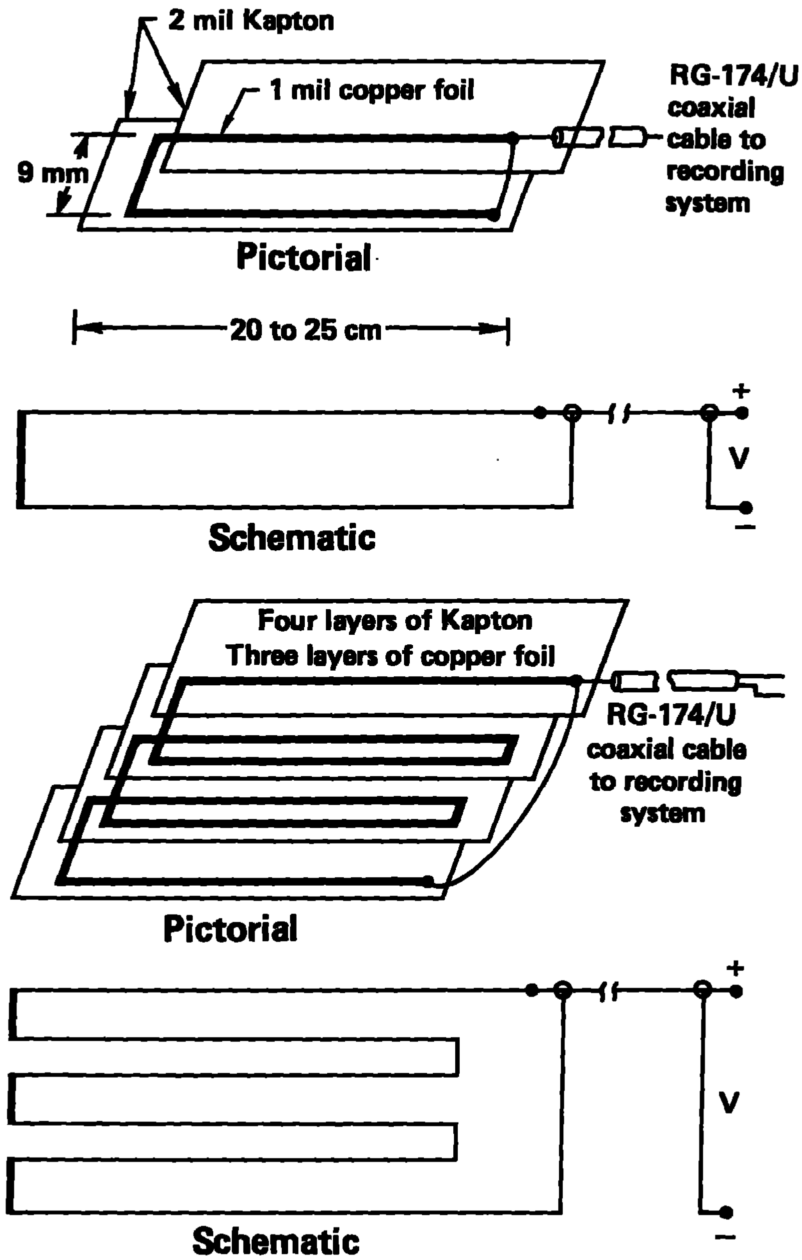

Spataro – Fig. 5

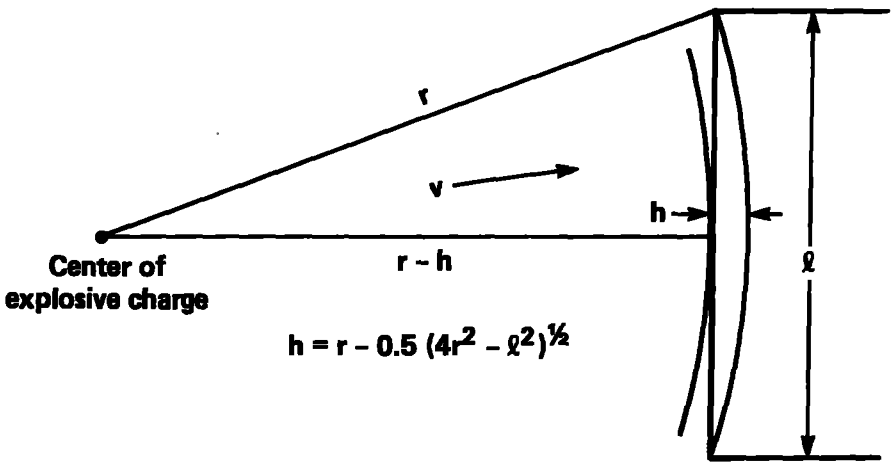

Spataro — Fig. 6

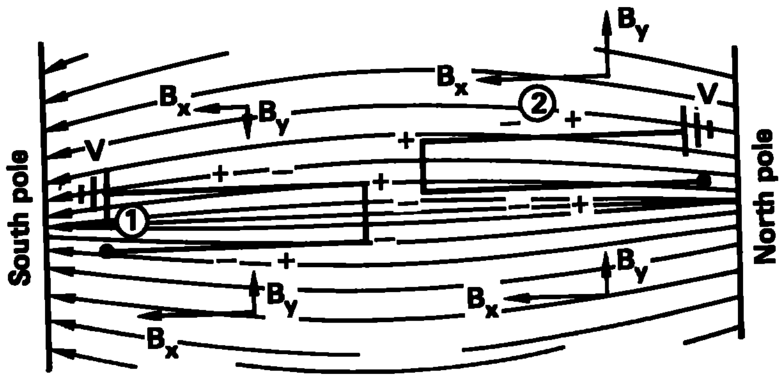

Spataro — Fig. 7

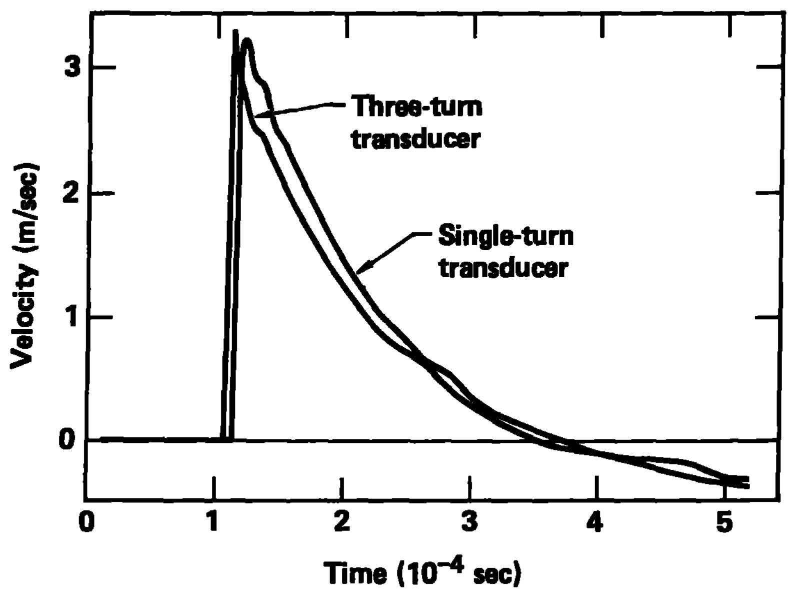

Spataro — Fig. 8

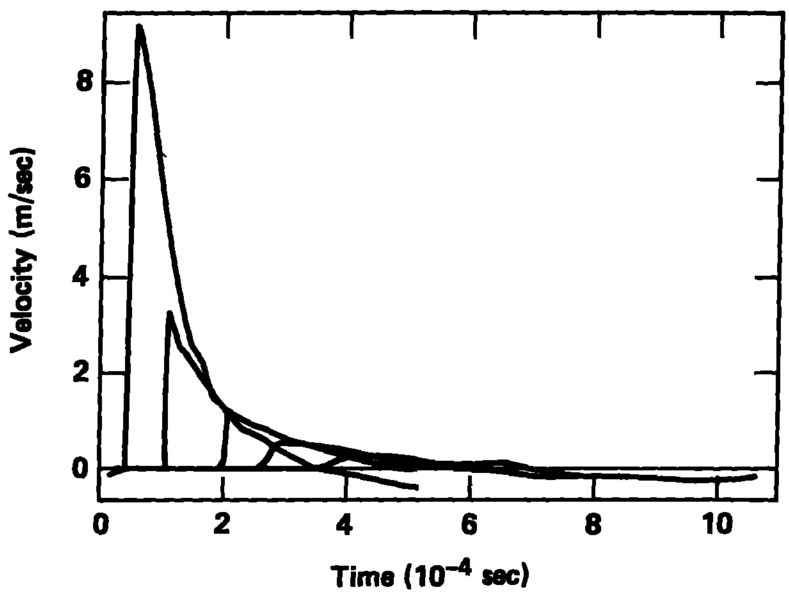

Spataro — Fig. 9